

Article

Distinct and Quantitative Validation Method for Predictive Process Modeling with Examples of Liquid-Liquid Extraction Processes of Complex Feed Mixtures

Axel Schmidt  and Jochen Strube *

Institute for Separation and Process Technology, Clausthal University of Technology, 38678 Clausthal-Zellerfeld, Germany; schmidt@itv.tu-clausthal.de

* Correspondence: strube@itv.tu-clausthal.de

Received: 18 March 2019; Accepted: 13 May 2019; Published: 19 May 2019



Abstract: As of today, industrial process development for liquid-liquid extraction and scale-up of extraction columns is based on an experimental procedure that requires tests in pilot-scale. This methodology consumes large amounts of material and time and the utilized scale-up equations are crude estimates including considerable safety margins. This approach is practical for well-known systems or low-value products coupled with high production scale, where such a scale-up methodology has less impact on the overall profitability. However, for new high-value products in biologics manufacturing, a process development based on process understanding and the use of validated process models is imperative. Therefore, a distinct and quantitative validation workflow for liquid-liquid extraction modeling is presented on the example of two complex feed mixtures. Monte-Carlo simulations based on the presented model parameter determination concept result for both examples in prediction accuracy comparable to the experiments and prediction precision within the deviation of the respective experiments. Identification of statistically significant parameters is demonstrated. The presented methodology for model validation will support the implementation of liquid-liquid extraction in the manufacturing of new high value biological products in regulated industries by providing a workflow to derive a Quality-by-Design compatible process model.

Keywords: liquid-liquid extraction; atpe; modeling; simulation; validation; verification; monte-carlo; design-of-experiments; quality-by-design; biologics

1. Introduction

The application of liquid-liquid extraction (LLE) is widespread in the chemical industry. It is often applied in areas, where distillation is not feasible. Prominent examples are the separation of organic compounds from aqueous feeds, e.g., phenols from waste water, or the separation of non-volatile components, e.g., metal ion extraction in hydrometallurgy, the recovery of caprolactam from nylon manufacturing and the wet purification of phosphoric acid [1,2]. However, especially in biologics manufacturing and in regulated industries in general, LLE is rarely part of the process chain, although it was shown in numerous cases to offer decisive advantages in terms of capacity, ease of scale-up, continuous operation and costs [3–8]. This is mainly due to a lack of knowledge regarding the practical aspects of this technology. This includes multistage operation and scale-up. Multistage operation in extraction columns is the common approach to maximize efficiency. How to perform the process development and especially the scale-up aspects of this technology are not widely known, except for supplier industry and some parts of academia, mainly institutes that conduct research in the field of process engineering with a focus on modeling. Furthermore, the current industrial practice

of scaling-up extraction columns is heavily reliant on pilot-scale experiments, which are time and material consuming [2,9,10]. While this alone is already a challenge to be overcome, for biologics manufacturing the more critical outcome is, that those methods are by nature empirical. Thus far, no prediction is possible due to the lack of process understanding, and therefore, no link between process and quality aspects can be made. This prevents current industrial process development practice for Quality-by-Design (QbD).

QbD-based process development is becoming the standard for new pharmaceutical products, such as virus-like-particles, plasmid DNA, fragments, etc., since it ensures quality through the whole lifecycle and allows, even demands, changes to the process after filing when optimization potentials occur, and because no comparable platform processes exist, as for monoclonal antibodies [11–14].

The application of QbD-principles for process development however requires a validated design space that guarantees constant quality, which can either be developed by experiments or by process understanding. Neither the pilot-based experimental method nor common scale-up equations are applicable for this purpose of resource efficient design space validation. Hence, there is a need for predictive LLE process models as well as a reliable workflow that distinctively and quantitatively validates prediction precision and accuracy. Sixt et al. [15] demonstrated the concept with an example of solid-liquid extraction (SLE). Here, we demonstrate it using an example of LLE.

The overall development workflow for a QbD-derived process is shown in Figure 1. In the beginning, a quality target product profile (QTPP) must be derived. This is necessary to define what is critical for product quality. Characteristics for biologics are for example sterility and purity, but also certain therapeutic effects, bioactivity and dosage. Depending on the QTPP critical quality attributes (CQAs) are to be defined, which is a property or characteristic that ensures desired product quality when controlled within a defined limit, range, or distribution [12,16]. In accordance with the QbD-philosophy, CQAs are dynamic rather than static and have to be updated during the lifecycle of products, when newly developed product and process knowledge suggest so. CQAs guide the further process development and are derived by risk management and experimentation.

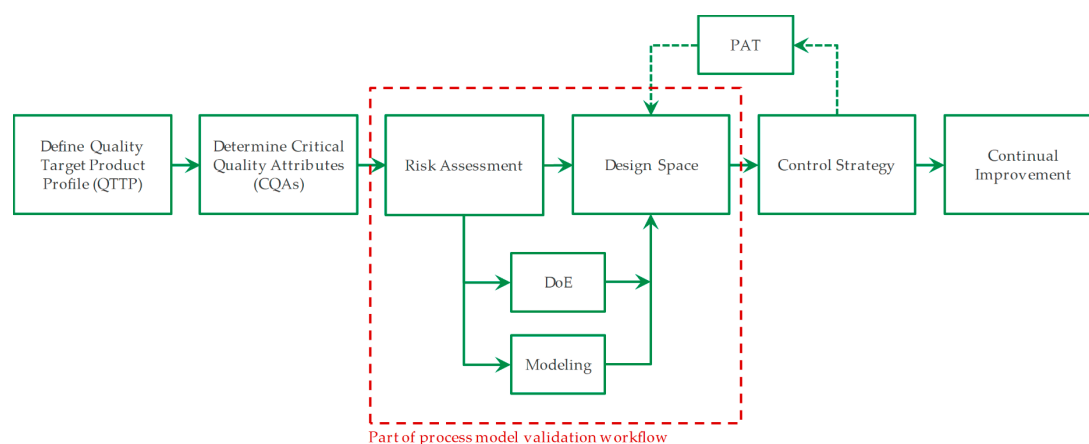


Figure 1. Process model validation workflow and its position in the overall Quality-by-Design (QbD)-based process development strategy. Adapted from [13]. After the definition of the quality target product profile and determination of critical quality attributes, risk assessment and design space identification can either be obtained by experiments or by modeling.

Risk assessment is part of the risk management and should be performed early in process development. Its purpose is to establish known and hypothetical links between material, equipment and process parameters and CQAs, setting the range of the further process design. Common tools for this, that are also suggested by the FDA (U.S. Food and Drug Administration), EMA (European Medicines Agency), PDA (Parenteral Drug Association) and ICH (International Council for Harmonisation of Technical Requirements for Pharmaceuticals for Human Use), are the construction of Ishikawa

diagrams, also known as fishbone diagram, and the performance of a failure-mode-effect-analysis (FMEA) [17]. Both are shown in Figure 2. The Ishikawa diagram basically summarizes different groups of effects, e.g., properties of materials, equipment design and process parameters that can represent a risk to certain CQAs, such as yield, purity or processability in general. The major branches are fanned out into minor branches, which reveal a more detailed causality between potential cause and risk. The degree of detail is only dependent on the amount of prior knowledge that the process development team has gathered. This diagram can already reveal critical process parameters (CPPs) that must be kept within a certain range during the process, and therefore should be part of process control strategy and might be needed to be investigated in more detail.

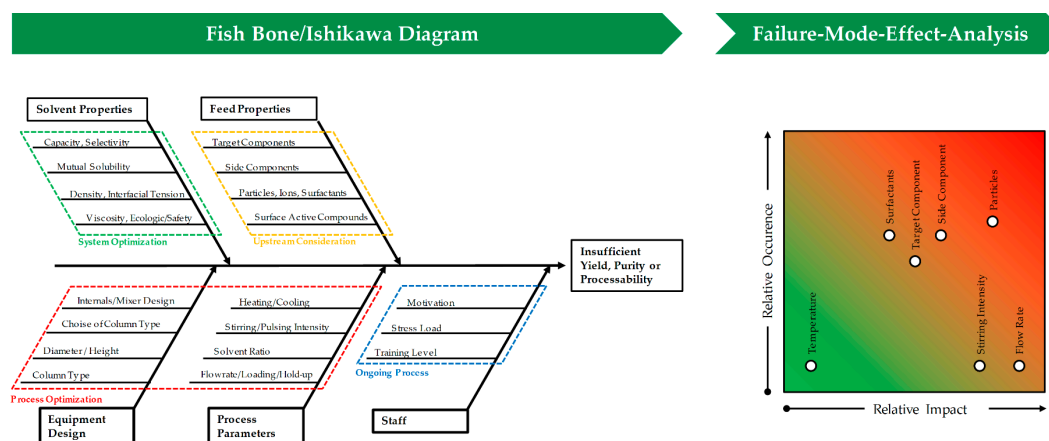


Figure 2. Construction of Ishikawa diagram and corresponding FMEA (failure-mode-effect-analysis) visualization are key-steps in risk assessment in a Quality-by-Design based process development.

A more quantitative tool during risk assessment is the FMEA. It is summarized in Table 1, graphically represented in Figure 2 and is derived by scoring the range of possible CPPs, identified in the Ishikawa diagram, regarding the possible impact that an occurring risk will have on quality attributes and the possibility that the risk will occur in the process of a stirred extraction column. It may be useful to include the chance of detecting the occurrence into the score. It is also possible to link certain parameters to each other, to also score potential interactions; however, this requires an even vaster prior knowledge about the system properties, which is seldom the case and therefore not shown here. Regarding LLE stirring intensity, in agitated columns, and the amount and presence of unwanted particles both can have a significant effect on process performance. While higher specific energy input causes an increase in hold-up, particles often hinder the coalescence of small droplets [18]. If not controlled and kept within a certain range, both can lead to column flooding, and therefore pose a high risk to the process stability. However, while the range of energy input is efficiently controlled by operating only at certain stirring rates, the occurrence of unwanted particles can easily be missed, if turbidity measurement of the feed or robust filtration is not part of the process and control strategy. This early risk management also offers guidance for the general process development, as for this example it already highlights settling-properties as key aspects during solvent selection.

Table 1. The failure-mode-effect-analysis (FMEA) for the process development of a stirred extraction column is derived by scoring the range of possible critical process parameters (CPPs), identified in the Ishikawa diagram, regarding the possible impact that an occurring risk will have on quality attributes and the possibility that the risk will occur.

Risk	Severity	Occurrence	Comment
Surfactants	4	6	Depending on type, can hinder coalescence. Is expected to be well controlled, once characterized in feed.
Temperature	1	1	Only affects coalescence, equilibrium and mass transfer beyond limits that will not occur in the process.
Particles	8	6	Occur very often. Depending on prior unit operations and control strategy. Can even be formed during extraction and hinder coalescence. Can cause flooding.
Target Component Concentration	5	5	Is expected to be in good control, once characterized in feed. However, it is a subject of natural feed variability and must be controlled to avoid oversaturation or yield loss.
Side Component Concentration	6	6	Is expected to be well controlled, once characterized in feed. However, it is a subject of natural feed variability and must be controlled to avoid inefficient purification or underperformance of following separation steps.
Stirring Intensity	8	1	Can easily lead to flooding if set too high or underperformance if set too low, since it is mainly responsible for hold-up and column efficiency. However, stirring can be very well controlled.
Flow Rate	9	1	Can easily lead to flooding if set too high or underperformance if set too low, since the solvent ratio besides power input is responsible for hold-up and column efficiency. However, flow rates can be very well controlled.

Looking back at the overall QbD-based process development strategy (Figure 1) reveals that the next steps are focused on determining the design space. Traditionally this is done solely based on experiments. To reduce the huge experimental effort, Design-of-Experiments (DoE) methods are usually applied. Even then, the amount of raw feed material necessary in the early process development stage might already be a criterion not to choose extraction technology for high-value products or lead to an experimental design that is limited to the fewest number of experiments possible or even eliminates the possibly more efficient unit-operation altogether, since there simply is not enough material at this stage to run the necessary tests. The development of a process-analytical-technology (PAT) supported control strategy and the continual improvement are the last steps in process development strategy, but they are beyond the scope of this work. More details regarding PAT-supported control strategies and continual improvement can be found in Kornecki et al. [19].

Predictive process models are the key-enabling tool to find a quantitatively defined and knowledge-based process optimum and design-space. They accelerate process development and at the same time generate process knowledge. They help to reduce the experimental effort and their validity does not end in the filed design space due to the physico-chemical nature of predictive process models. Each model that is to be utilized in this manner must be proven to be at least as accurate and precise as the respective experiments it ought to substitute. This requirement leads to the workflow for process development and validation as shown in Figure 3. First introduced by Sixt et al. [15], it is based on four distinct decision criteria for each development and validation phase [14,15].

First, the model task and its application must be defined. In case of LLE, the concentration profile in the extraction column must be correctly predicted by taking all effects (fluid dynamics, phase equilibrium and mass transfer kinetics) into account. Combining prior knowledge and studying existing literature results in the derivation of the appropriate model approach and depth. Simply,

mass and energy balance checks on the example of simplified case-studies are sufficient to decide, if the conceptual model is verified.

Second, the sensitivity of the model must be investigated. Therefore, one-parameter-at-a-time studies can reveal if the model behaves in a way to be expected by an experienced process engineer. Therefore, step size of variable change should be rather large to exemplify parameter effects. However, multi-parameter-at-a-time studies are more suitable to quantify sensitivity. By applying DoE-principles a screening design can serve as plan for simulation studies. The investigated space should in contrast to one-parameter-at-a-time-studies be within the system specific boundaries, e.g., the solvent ratio in an extraction column is limited by the mutual solubility, as is the maximum loading limited by the density difference between both phases. Details on the sensitivity analysis are given in Section 4.1.

Third, field experiments at specific points of the DoE simulation must be done, in order to compare precision and accuracy of the model at different operating points to the experiment. Last statistical evaluation such as PLS (partial-least-squares) loading plots help to quantify the results from the simulation studies.

The objective of this article is to present the complete walkthrough using an example of a monoclonal antibody and Artemisinin, both representing products from highly non-ideal complex multicomponent mixtures for regulated industries.

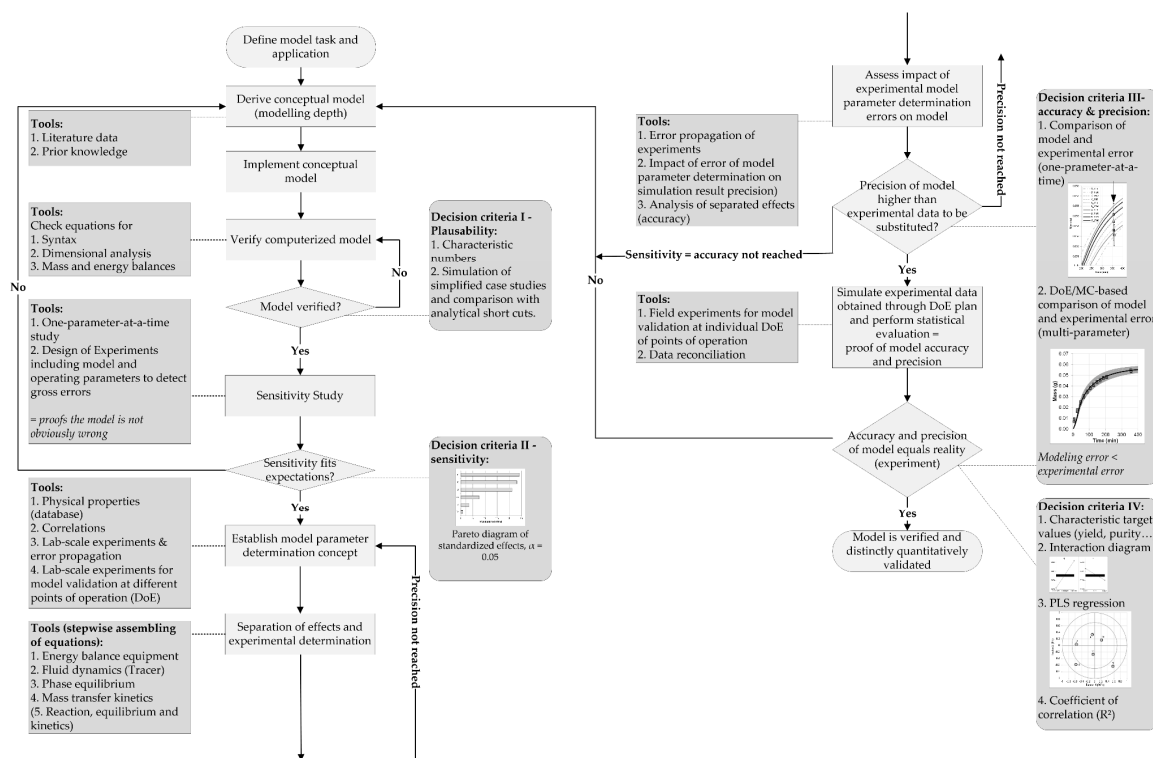


Figure 3. Workflow scheme for process model development and validation. Adapted from [15].

2. Modeling Liquid-Liquid Extraction

The use of LLE as a separation process was already known before the 19th century to produce dyes, fragrances and pigments. The basic theories of equilibrium distribution were laid by Berthelot and Jungfleisch [20] as well as Nernst [21]. These findings were soon followed by the first industrial applications, such as countercurrent configuration, and technical developments, such as stirred extraction columns [22].

The methods developed for the design of processes in the first half of the 20th century still exist today in industrial practice. Major milestones before 1950 were the introduction of mass transfer coefficients by Lewis [23], stage construction and graphical methods in equilibrium representations

by McCabe and Thiele [24], Kremser [25] and Hunter and Nash [26], as well as the concept of solute transfer units introduced by Colburn [27].

In the 1950s, progress was made in identifying fluid dynamics as a major contributor to the effects that are crucial in predicting LLE in technical applications. The fact that there is a large deviation from plug-flow regime in extraction columns, and therefore a diminished efficiency, was made by Geankoplis and Hixson [28], Burger and Swift, Sege and Woodfield [29] and Thornton and Logsdail [30]. Danckwerts [31] introduced the axial dispersion model (ADM) as a mathematical description of plug-flow overlapped by backmixing. Alongside with other researchers Levenspiel and Smith [32], Sleicher [33] and Stemerding and Zuiderweg [34] were on the forefront in contributing to this model concept, developing methods to determine the dispersion coefficient and to quantify the effect of axial dispersion on separation efficiency.

In the 1960s, Miyauchi and Vermeulen [35] were among the first to apply the DPF model and calculate concentration profiles in extraction columns. Additionally, limitations of this model approach were discussed, among others by Rod [36], who introduced the term “forward-mixing”, partially caused by so-called channeling.

From the 1970s to the 1980s, many working groups discussed if deviation from plug flow, caused by different convective velocities of drop size distributions, can be represented by the axial dispersion model. A summary of available model approaches developed during this period was done by Steiner and Hartland [37]. While some researchers found good agreement with axial dispersion model predictions and experimental data like Reissinger [38], the development of models that specifically account for coalescence and breakage of drops by population balance models (PBM) began. Jirnicy et al. [39,40], Cassamata and Vogelpohl [41], Haverland et al. [42], Al Khani et al. [43], Cruz-Pinto and Korchinsky [44], Coualaloglou and Tavlarides [45], Tavlaritis and Bapat [46] and Hamilton and Pratt [47] were the major contributors to develop and expand on this model type. The three major modeling approaches to LLE in extraction columns at this point in time and their respective system boundaries are shown in Figure 4.

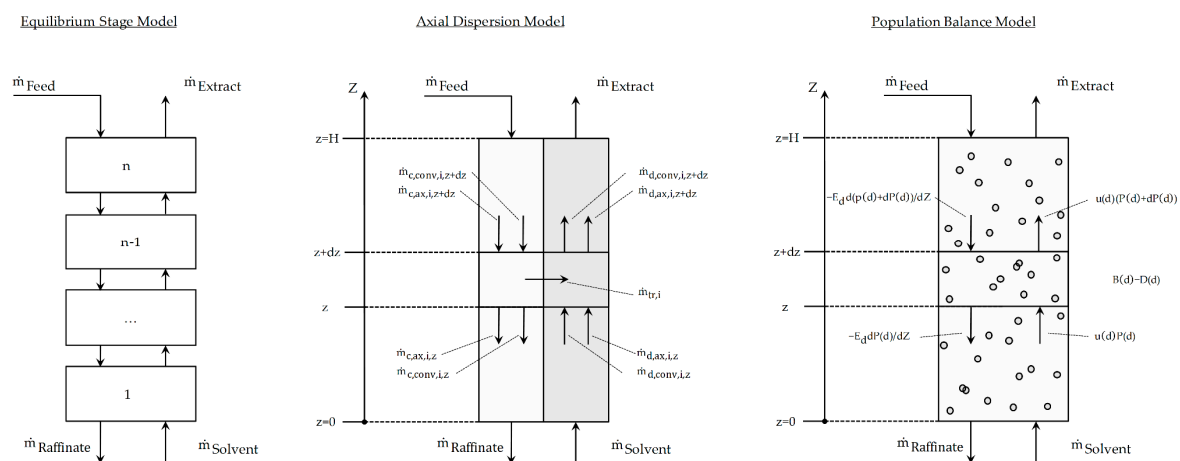


Figure 4. Model balance volumes for distributed plug flow model and schematic comparison to stage and population balance model approach.

In the 1990s, computational capacities increased significantly, and thus, many research groups focused their research development on PBM and more sophisticated kernels to calculate coalescence and breakage in more detail. Major contributions were made by the research groups of Bart and Pfennig, for example in the work of Kronberger et al. [48] and Henschke et al. [49].

More recently, research began to focus on the fact that the increase in model depth had to be supplemented by parameter determination concepts in order to be predictive. Among others, Hoting [50] published model prediction for the EFCE (European Federation of Chemical Engineering)

standard test system water, butyl acetate, acetone in packed extraction columns. The project “from single-drop to extraction column” focused on PBM approaches and could show for packed and agitated columns scale-up was possible on the example of the EFCE standard test systems [51–53].

Franke et al. [54], Leistner [55], Eggersglüß [5–7] and Wellsandt [56] from the research group of Strube worked on parameter determination concepts for complex feed mixtures and demonstrated the feasibility of model based process development. Since then, some research dives even deeper into modeling depths by combining CFD with PBM [57]. However, for industrial use and the prediction of processes including complex feed mixtures, the axial dispersion model still is the approach of choice, due to accounting for all relevant effects and also the availability of more precise and efficient model parameter determination concepts.

Axial Dispersion Model

The fundamental equations of the axial dispersion-model are based on the transport equations for the continuous (see Equation (1)) and the dispersed phase (see Equation (2)). They describe the mass balance around the system boundary as shown in Figure 4 (middle). The accumulation term on the left hand side of the equations is the sum of the change in concentration due to the convective mass flow, mainly characterized by the velocity u , the dispersed mass flow, mainly characterized by D_{ax} , and the mass transfer between both liquid phases depend on the effective mass transfer coefficient k_{eff} , hold-up, sauter diameter d and equilibrium concentration $c_{i,Eq}$:

$$\frac{\partial c_i^c}{\partial t} = -u_c \cdot \frac{\partial c_i^c}{\partial z} + D_{ax}^c \cdot \frac{\partial^2 c_i^c}{\partial z^2} + k_{eff} \cdot \frac{\Phi}{(1-\Phi)} \cdot \frac{6}{d} \cdot (c_i^d - c_{i,Eq}^d) \quad (1)$$

$$\frac{\partial c_i^d}{\partial t} = u_d \cdot \frac{\partial c_i^d}{\partial z} + D_{ax}^d \cdot \frac{\partial^2 c_i^d}{\partial z^2} - k_{eff} \cdot \frac{6}{d} \cdot (c_i^d - c_{i,Eq}^d) \quad (2)$$

In the extraction columns, there is a deviation from the ideal plug flow due to back-mixing. This leads to a deviation from the ideal residence time distribution and thus to different contact times between the dispersed and the continuous phase. The result is a decreased separation efficiency [6,7]. This so-called dispersion can be characterized by the axial dispersion coefficient D_{ax} , which is either experimentally determined for the continuous and the dispersed phase by tracer tests or by corresponding empirical correlations. Depending on the column type and internals different correlations are published. For the continuous phase, the approach in Equation (3) is often applied:

$$D_{ax}^c = u_c \cdot H_c \cdot \left(C_1 + C_2 \cdot \left(\frac{D_R \cdot N}{u_c} \right) \cdot C_3 \right) \quad (3)$$

In addition to the stirrer diameter (D_R) and the stirrer speed (N), the Equation also contains the constants (C_1 , C_2 and C_3), which account for different geometries of stirrer and column. Therefore, the coefficients are selected according to the column type, its diameter and overall stirrer geometry [58–61]. A modified correlation from Rod and Misek for the axial dispersion coefficient of the dispersed phase for Kühni columns can be seen in Equation (4) [62]. As for the continuous phase, there are several correlations published that are determined for specific column scales and geometry [63–65].

$$D_{ax}^d = \frac{1}{Bo} = 0.056 + 1.19 \cdot 10^{-2} \cdot \left(\frac{d_R \cdot N}{u_d} \right)^{3.45} \quad (4)$$

The cross-sectional column loading (L) is another important parameter for the characterization of column efficiency. It is defined as the sum of the volume flows of the continuous (V_C) and the disperse phase (V_D) divided by the column cross-sectional area (A_C):

$$L = \frac{V_D + V_C}{A_C} \quad (5)$$

The corresponding differential equations can be solved by the implementation of two boundary conditions for the continuous and dispersed phase, which are shown in Equations (6) and (7):

$$\frac{\partial c(z=L)}{\partial z} = 0 \quad (6)$$

$$D_{ax} \cdot \frac{\partial c(z=0)}{\partial z} = u \cdot (c(z=0) - c_{in}) \quad (7)$$

3. Model-Parameter Determination

For the application of the axial dispersion model in process design, the determination of a set of model parameters is necessary as described in the section before. Ideally, the complete set of parameters can be determined with as few experiments as possible and thus with as little material and time as possible. However, this requires a standardized and effect oriented model parameter determination concept. The workflow to determine model parameters, which are needed for the DPF-model, is shown schematically in Figure 5.

Modeling Recipe of Liquid-Liquid Extraction Processes

▪ Distributed Plug Flow Model:

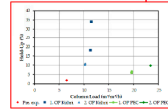
$$\text{Dispersed Phase MB: } \frac{\partial c_{d,i}}{\partial t} = -u_d \times \frac{\partial c_i}{\partial z} + D_{ax,d} \times \frac{\partial^2 c_i}{\partial z^2} + k_{eff} \times \frac{6}{d_{drop}} \times (c_{d,i} - c_{d,eq,i})$$

$$\text{Continuous Phase MB: } \frac{\partial c_{c,i}}{\partial t} = u_c \times \frac{\partial c_i}{\partial z} + D_{ax,c} \times \frac{\partial^2 c_i}{\partial z^2} - k_{eff} \times \frac{\varphi}{(1-\varphi)} \times \frac{6}{d_{drop}} \times (c_{d,i} - c_{d,eq,i})$$

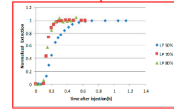
- 3 days to 1 week
- 100–200 g Feed material
- 3 Tracer velocities + rep.
- 5 Droplet sizes + rep.
- 5 Concentrations

▪ 1. Fluid Dynamics:

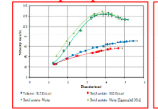
1.1 Column Hold-Up



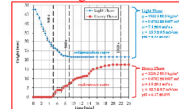
1.2 Tracer Experiments



1.3 Drop Experiments

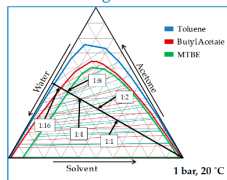


1.4 Settling Behavior

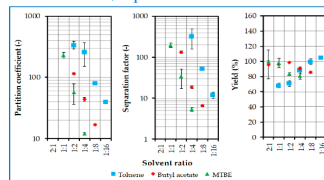


▪ 2. Phase Equilibrium:

2.1 Phase Diagram



2.2 Distribution/Separation Factors



▪ 3. Mass Transfer Kinetics:

3.1 Effective Mass Transfer Coefficient

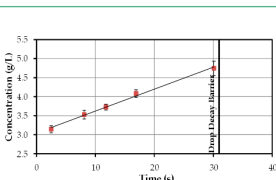


Figure 5. Modeling and parameter determination recipe scheme for liquid-liquid extraction processes.

The sequence to determine these parameters are ordered according to their importance and effect on the process:

1. Fluid dynamics (red): the fluid dynamic behavior of the system is dependent on the axial dispersion of the system, as well as on the hold-up (Figure 5, 1.1), characterized by drop rise velocity, droplet sauter diameter and column loading. The axial dispersion coefficient must be determined by tracer experiments (Figure 5, 1.2) if it is not to be determined by correlations. Since this parameter is primarily geometry-dependent, the actual feed solution does not have to be used. Around 2–5 L of total system volume, depending on the investigated scale, is required for the determination of axial dispersion behavior. A qualified person can perform this experiment within 1 day.

A droplet measurement cell can be used for the quantification of the drop size and drop rise velocity (Figure 5, 1.3), which is dependent on the sauter diameter. Few milliliters, up to 50 mL, are required to determine this parameter within 1 to 5 days. Batch-settling experiments to determine the settling time and properties of the system can add additional information regarding which solvent to choose for the process (Figure 5, 1.4); however, they are not mandatory for the parameter determination.

2. Phase equilibrium (blue): shaking flask experiments must be performed to determine the binodale, tie-lines and distribution coefficients of target and main side components. Up to five points evenly spread around the phase diagram can typically deliver the necessary information. Between 5 and 10 mL are usually enough per shaking flask experiment to determine these parameters. However, if interfacial tension, viscosities and densities for both phases are not known or accessible by reliable database or correlation, the volume should be increased to obtain these data also from the shaking flask experiments. If determined in triplicates, 75 ($3 \times 5 \times 5$ mL) up to 150 ($3 \times 5 \times 10$ mL) mL of system volume are needed for the quantification. Up to 2 days are sufficient for execution.

3. Kinetics (green): the effective mass transfer coefficient is necessary to correctly describe the kinetic of the extraction process. Lower values of this parameter result in more time necessary for component separation. This parameter can also be quantified by droplet measurements, and thus, should be determined parallel to the drop measurements during the 1 to 2 days period.

The time and material resources necessary for a complete model parameter determination as described above requires around 3 days up to 1 week and only 200 up 300 mL feed material. More detail for each model parameter experiment can be found in [66].

4. Model Validation

In the following subsections, we show the decisive steps during the model validation. First, syntax, mass and energy balance must be checked. It is advisable to also test if the principle model behavior is logical, e.g., that mass transfer direction is correct. Exemplary case studies, either from in-house data or from literature can help to identify a suitable reference point and to show that the model is not obviously wrong.

4.1. Sensitivity Analysis

As described in the introduction, the next steps are one-parameter-at-a-time sensitivity studies. Here, data from Hoting [67] were used as point of reference. The parameters for the sensitivity analysis are shown in Table 2. It was investigated how big the influence of each parameter is, when the others are kept at their default value. Figure 6 shows the result for the first sensitivity study. The mass flow of the dispersed and continuous phase affects the concentration profile the most. This is to be expected, as they determine the solvent ratio and whether the feed stream is depleted from the solute by the solvent stream or whether the solute quickly reaches equilibrium concentration in the solvent stream. The distribution coefficient has a default value of approximately 1. Thus, a variation of this parameter of 30% is enough to induce a change of the concentration profile similar to the effects of the solvent ratio. The other parameters, such as hold-up, sauter diameter and axial dispersion, only show small influences on the concentration profile when kept within reasonable values (see Table 2).

Table 2. Axial dispersion model parameters for the one-parameter-at-a-time sensitivity analysis.

Model Parameter	Unit	Deviation
Mass flow continuous phase	kg/h	58–109 ($\pm 30\%$)
Mass flow dispersed phase	kg/h	63–118 ($\pm 30\%$)
Distribution coefficient	-	0.84–1.18 ($\pm 30\%$)
Mass transfer coefficient	m/s	$7.5 \times 10^{-6} - 1.2 \times 10^{-4}$
Axial dispersion continuous phase	m ² /s	$3 \times 10^{-7} - 1.2 \times 10^{-4}$
Axial dispersion dispersed phase	m ² /s	$3 \times 10^{-7} - 1.2 \times 10^{-4}$
Sauter diameter	mm	1–7 ($\pm 75\%$)
Hold-up	-	0.045–0.36 ($\pm 75\%$)

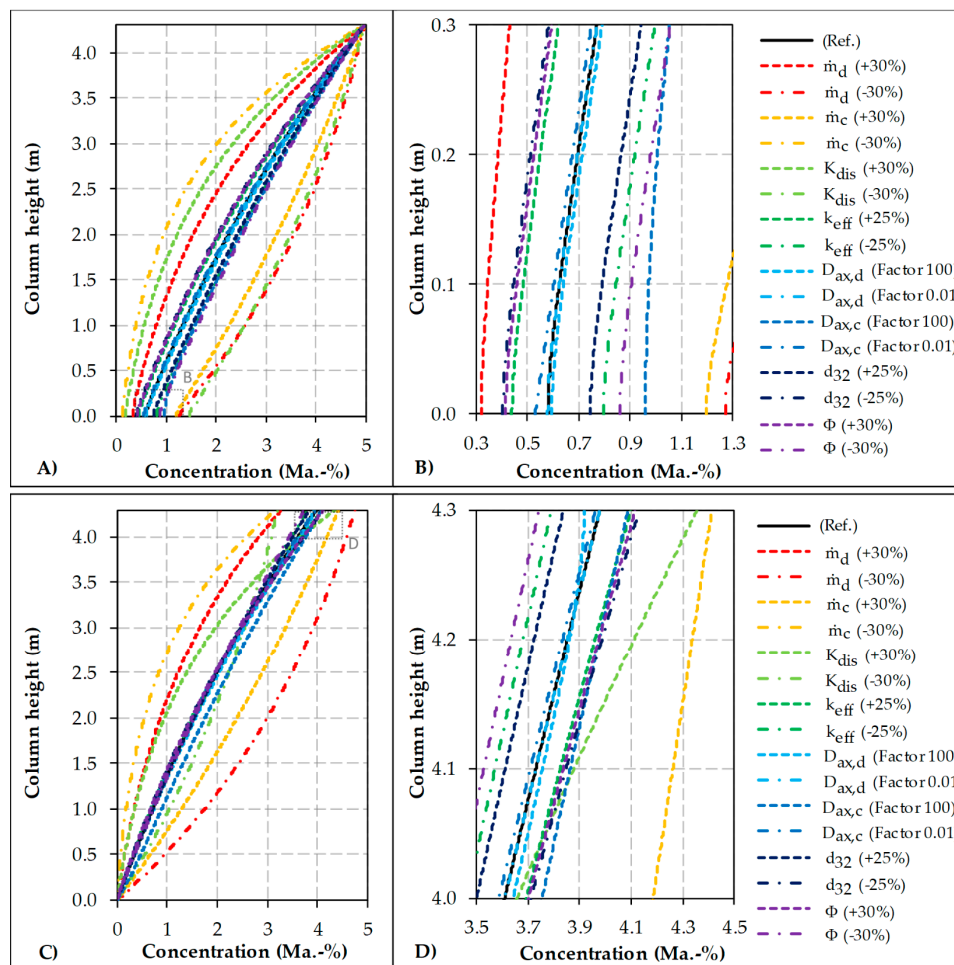


Figure 6. One-parameter-at-a-time sensitivity study. (A,B) Concentration profile of the continuous phase. (C,D) Concentration profile of the dispersed phase. The strongest impact on the concentration profile is achieved by altering the mass flow of the continuous, the dispersed phase and the distribution coefficient of acetone. (B,D) On the right hand side are insets of (A,C).

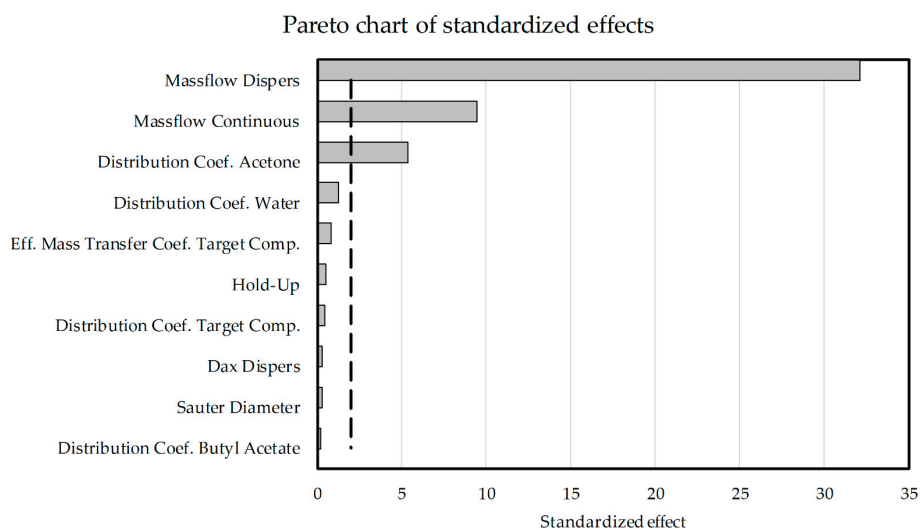
The next step during sensitivity analysis is the performance of multi-parameter-at-a-time studies. This reveals parameter combinations that have a significant effect on a CPP such as purity or concentration. Therefore, it is recommendable to apply a DoE-derived simulation plan, which mimics the experiments plan otherwise necessary for optimal operation space identification. This will be shown in the following using as an example the purification of Artemisinin.

Table 3 summarizes the Plackett-Burman-Design for the simulation studies, which is typically used in the early process development stage to screen for the most important factors that influence the process outcome [68]. The combined mass flow of the continuous and dispersed phase are limited by the flooding point of the system, which was determined to be around $12 \text{ m}^3/\text{m}^2/\text{h}$, the minimum solvent ratio. The concentration of Artemisinin and the side components are variable due to the natural raw feed material variability. The other parameters are set within the range of what can occur during the process.

Table 3. Axial dispersion model parameters for the multi-parameter-at-a-time sensitivity analysis.

Parameter	Unit	Min	Center	Max
Mass flow continuous phase	kg/hr	3	3.58	4.2
Mass flow dispersed phase	kg/hr	0.5	1.13	1.9
Concentration Artemisinin	kg/m ³	0.7	0.84	1
Concentration side components	kg/m ³	1.2	1.53	1.85
Dispersion coefficient	m ² /s	8.50×10^{-5}	1.08×10^{-4}	1.30×10^{-4}
Distribution coefficient acetone	-	1	1.3	1.6
Distribution coefficient Artemisinin	-	30	90	150
Distribution coefficient side components	-	0.1	1.3	2.5
Effective mass transfer coefficient	m/s	2.00×10^{-5}	2.50×10^{-5}	3.00×10^{-5}
Hold-Up	-	0.16	0.18	0.2
Sauter diameter	mm	3.5	4.5	5.5

Figure 7 shows the Pareto chart of standardized effects obtained from the simulation runs. The statistical criterion of significance here is the p-value. If the model parameters are evaluated by the increase in Artemisinin concentration; then, it becomes clear that the massflow of the continuous and dispersed phase are the most significant factors. Since the distribution coefficient of Artemisinin is comparably high, mass transfer is fast and equilibrium composition is reached very quickly. Larger deviations of other parameters that influence mass transfer, such as the effective mass transfer coefficient, sauter diameter and hold-up become therefore non-significant. Thus, the concentration of Artemisinin is mostly determined by the solvent ratio. The third significant parameter is the distribution coefficient of acetone. This is also easy to understand, since acetone is also a solute that is extracted, however in much larger quantities. The more acetone is extracted, the larger the extract volume gets and the more diluted the Artemisinin concentration becomes.

**Figure 7.** Results of multi-parameter-at-a-time sensitivity study that reveal statistically significant model parameters. Parameters that cross the reference line (dashed) are statistically significant.

4.2. Statistical Evaluation

The last steps in the model validation workflow presented here include the statistical evaluation of different operating points of the previously simulated DoE. First, the center point of the statistical simulation plan is established; second, selected optimized operating point is evaluated with regard to precision and accuracy. Finally, the simulation of an aqueous two-phase extraction in a packed extraction column serves to present the robustness of the model, which explicitly includes the secondary component profile.

Figure 8 shows the results of the center point simulation (left) and the simulation of the optimized operating point (right) compared to the experiment. Data represent experimental duplicates as well as the standard deviation. Since all model parameter determinations are subject to statistical and methodological error, these must be taken into account in the simulation to enable a reliable comparison to the experiments. This is achieved by the random, evenly distributed variation of the model parameter values in a Monte-Carlo simulation. The default values are the results obtained from the model parameter determination. The range of deviation is determined from the error calculation for each model parameter. The default values and the range of deviation for the simulation are summarized in Tables 4 and 5. All process information in detail can be found in our previously published work [69].

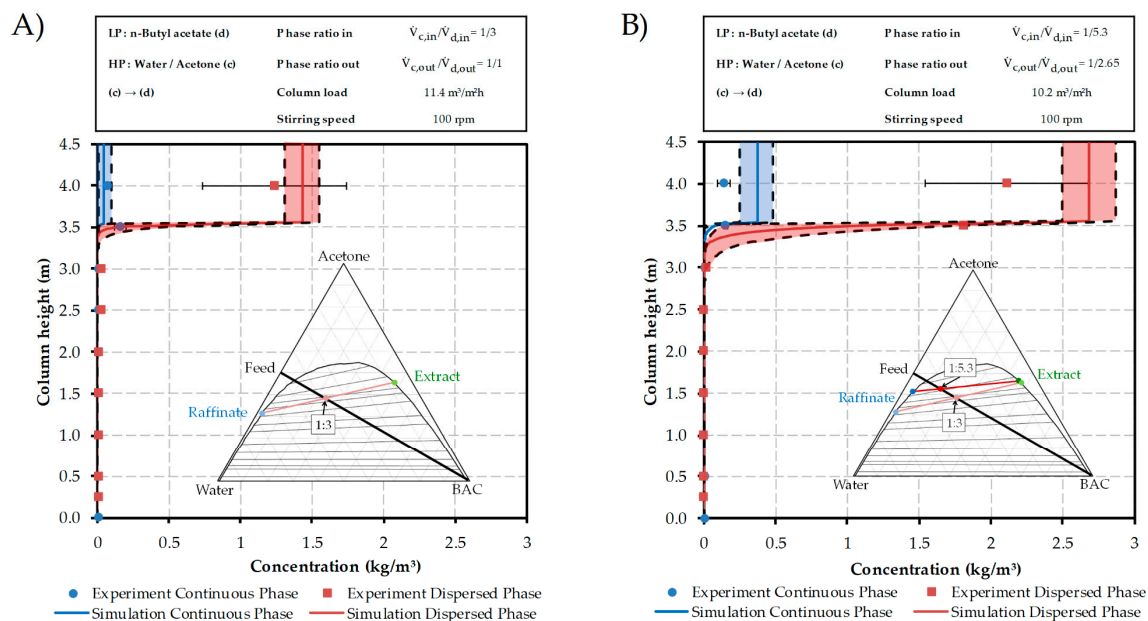


Figure 8. Comparison of experimental and simulated column profiles. Center-point is shown on the left side (A), the optimized operating point is shown on the right hand side (B). The enveloped curves represent the minimum and maximum values of 100 Monte-Carlo simulation runs. Also shown are the phase diagrams including mixing point, extract and raffinate composition for each operating point.

Table 4. Axial dispersion model parameters for the center point study. The default values of the simulation equal the experimental process parameters.

Parameter	Center Point	Unit	Default	Deviation
Mass flow continuous phase		kg/h	3.58	± 0.0252
Mass flow dispersed phase		kg/h	1.13	± 0.0546
Concentration Artemisinin		kg/m ³	0.84	± 0.02
Dispersion coefficient		m ² /s	1.08×10^{-4}	$-9.80 \times 10^{-5} / +1.08 \times 10^{-4}$
Distribution coefficient acetone		-	1.3	± 0.13
Distribution coefficient Artemisinin		-	90	± 9
Effective mass transfer coefficient		m/s	2.50×10^{-5}	$\pm 1.25 \times 10^{-6}$
Hold-Up		-	0.18	± 0.045
Sauter diameter		mm	4.5	± 1.5

Table 5. Axial dispersion model parameters for optimized operating point study. The default values of the simulation equal the experimental process parameters.

Parameter Operating Point 2	Unit	Default	Deviation
Mass flow continuous phase	kg/h	3.6	±0.006
Mass flow dispersed phase	kg/h	0.64	±0.0168
Concentration Artemisinin	kg/m ³	0.87	±0.01
Dispersion coefficient	m ² /s	1.08 × 10 ⁻⁴	-9.80 × 10 ⁻⁵ /+1.08 × 10 ⁻⁴
Distribution coefficient acetone	-	1.3	±0.13
Distribution coefficient Artemisinin	-	30	±3
Effective mass transfer coefficient	m/s	2.50 × 10 ⁻⁵	±1.25 × 10 ⁻⁶
Hold-Up	-	0.18	±0.045
Sauter diameter	mm	4.5	±1.5

Both operating points are characterized by a high utilization of the column in the upper area. This fits with the previously discussed findings that the distribution coefficient of Artemisinin is so large that it is fully extracted at a very early stage in the process. Therefore, the resulting concentration value at the head is only significantly dependent on the set solvent ratio, which is specified as a process parameter and can thus be optimized, and the distribution coefficient of acetone underlying the system, which determines the volume of the extract phase. An example with a more evenly spread column profile is presented later.

The simplex (enveloped curves) represents the minimum and maximum values of 100 Monte-Carlo simulation runs. As can be seen the derived model precision is within the experimental deviations. If the accuracy of the model is compared to the experiments, the center point concentration can be very well predicted (left diagram (A) in Figure 8). The optimized operating point is derived from our previous work, that showed that the concentration can be increased by decreasing dispersed solvent mass flow towards the minimum solvent ratio, which is around 1/6 [69]. Herein, the increased concentration (experiment and simulation) can be easily observed, which underlines the correct parameter implementation. Furthermore, a larger deviation of the simulated and experimental head-concentration can be observed in the column height of 3.5 to 4.5 m. The model inherently closes the mass balance, which is due to error in analytics, experimental procedure and product instability not necessarily reflected in the experiment. The simplex is within the experimental deviation, and therefore the necessary model accuracy is given.

Since for the model purpose of replacing experiments specified in the introduction a sufficient precision and accuracy are given, model parameter influence can now be statistically evaluated. Figure 9 shows the partial-least-squares regression loading plot. The inner circle includes all model parameters (predictors, blue) that explain up to 50% of the observed variance. The area between the inner and outer circle contains the predictors that explain the remaining variance. Model parameters that are positively correlated to the here evaluated target component concentration (response, red) are located in the same direction of the diagram. For example, the mass flow of the continuous phase is positively correlated to the response, since its increase practically leads to more of the target component that can be extracted and indirectly decreases the solvent ratio. This is even better illustrated by the mass flow of the dispersed phase, which is located in the opposite direction of the target component concentration and therefore implies a negative correlation to the model response. This fits very well with all the above mentioned findings (sensitivity studies, Pareto-chart, comparison of experiment and simulation of two operating points, which origin from the DoE and theoretical understanding) and is the final step in the model validation workflow.

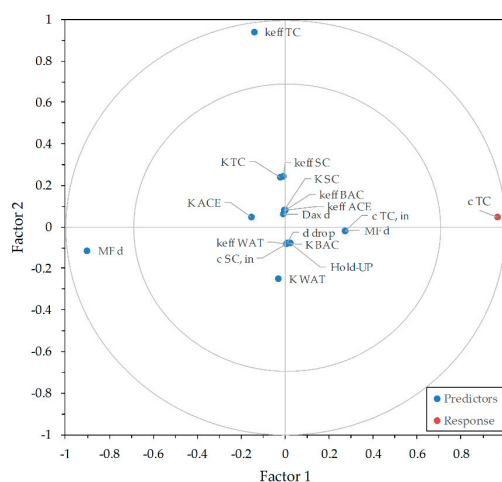


Figure 9. Partial-least-squares analysis of the model parameters used in the multi-parameter-at-a-time sensitivity study. MF (mass flow), K (distribution coefficient), k_{eff} (effective mass transfer coefficient), Dax (axial dispersion coefficient), d (diameter), TC (target component), SC (side component), ACE (acetone), BAC (butyl acetate), WAT (water).

It should be noted that for other systems both the Pareto and the PLS loading diagrams will be different. For example, for a mass transport-limited system the solvent ratio is expected to be far less significant. On the other hand, the smaller the distribution coefficient of the target component in the system becomes, the more significant its influence on the concentration profile is and it should be positively correlated to the extract concentration. The same rationale is applicable for the mass transfer coefficient. However, the procedures and methods of evaluation should always be based on the procedure and the evaluation criteria shown here in order to enable an evaluation of the validity of the model for use in a QbD-based process development as discussed in the introduction and depicted in Figure 1.

Finally, to further demonstrate the validity of the model, it is applied to the wash extraction of a monoclonal antibody (mAb). Details on the latter study are published by Eggersgluess et al. [7] and process parameters are summarized in Table 6. After capture of the antibody from a cell culture harvest by aqueous two-phase extraction, the mAb containing light phase is washed in multistage-operation with fresh heavy phase. The process is executed in a packed extraction column. The light phase enters the column dispersed at the bottom; the heavy wash phase enters the column as continuous phase at the top. For the design of the total process it is especially important to have information about the purity profile to be able to design the subsequent purification steps adequately. The size exclusion chromatogram of the inlet and outlet streams is shown in Figure 10. The monoclonal antibody (mAb) peak is located at around 10 min. The following peaks can be contributed towards lower molecular weight (LMW1, LMW2, LMW3, LMW4) components, which will serve in the following as the investigated impurities. The comparison between the experimental and simulated purity profiles is shown in Figure 11. The simulated purity profile for LMW1 and LMW4 are well within the experimental deviation. This is to be expected, since LMW1 does not show a high solubility in the continuous phase and LMW4 already is highly depleted at the column inlet. The more difficult impurities LMW2 and LMW3 are also within the experimental deviation at the column top, with larger deviations for LMW2 at the column middle. However, the critical overall purity profile is then again within the experimental deviations over the entire column length.

Table 6. Process and model parameters for the wash extraction from [7]. The default values of the simulation equal the experimental process parameters. The dispersed phase enters the column at the bottom; the continuous phase inlet is at the column top.

Parameter	Unit	Default	Deviation
Massflow dispersed phase	g/min	3	5%
Massflow continuous phase	g/min	15	5%
Density dispersed phase	kg/liter	1.118	5%
Density continuous phase	kg/liter	1.222	5%
Dispersion coefficient, dispersed	m ² /s	5.60×10^{-5}	10%
Dispersion coefficient, continuous	m ² /s	4.70×10^{-5}	10%
Sauter diameter	mm	0.21	10%
Hold-Up	-	0.2755	10%
Distribution coefficient mAb	-	100	5%
Distribution coefficient LMW1	-	15.23	5%
Distribution coefficient LMW2	-	4	5%
Distribution coefficient LMW3	-	3.5	5%
Distribution coefficient LMW4	-	1.83	5%
Effective mass transfer coefficient	m/s	1.00×10^{-6}	5%

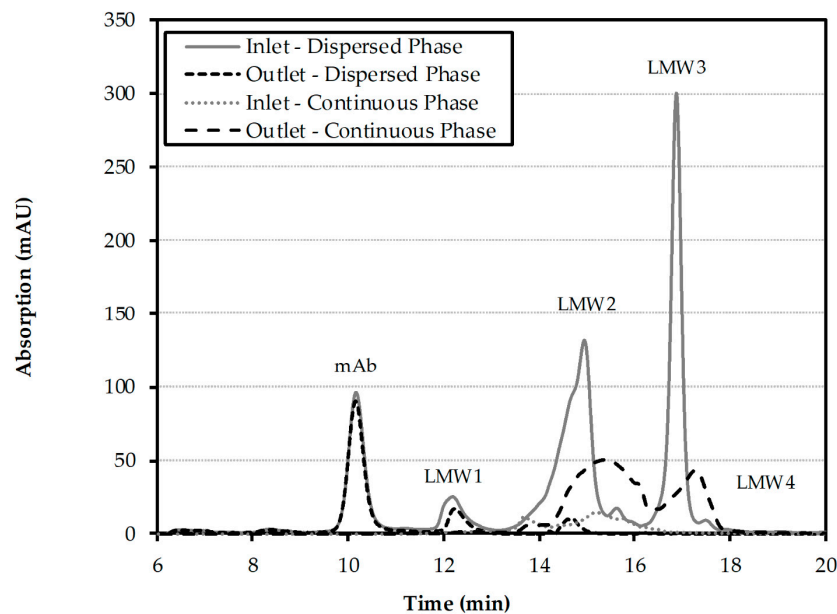


Figure 10. Size exclusion chromatograms of the inlet and outlet streams of the wash extraction [7].

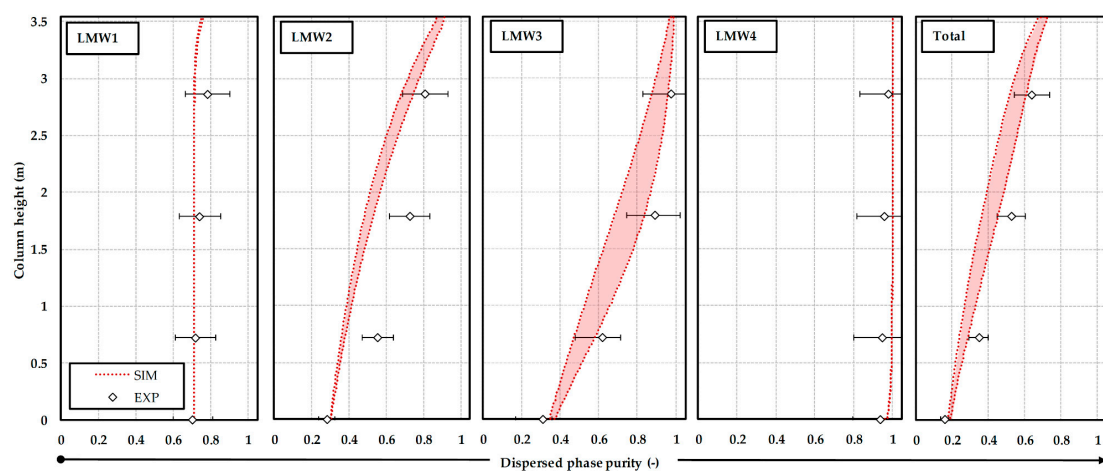


Figure 11. Comparison of experimental and simulated purity profiles of the wash extraction.

5. Material and Methods

The materials and methods for the Artemisinin study can be found in detail in our previously published article [69]. Butyl acetate for the column tests was purchased from ThermoFisher (Waltham, MA, USA) in technical grade purity of 99% (by GC). Acetone was purchased from VWR (Darmstadt, Germany). The analysis of artemisinin by HPLC is performed on an Elite LaChrom[®] device equipped with an Evaporation Light Scattering Detector (ELSD) Alltech[®] 3300 (Grace[®], Columbia, SC, USA). The analytical column is a PharmPrep[®] RP18 250 mm × 4 mm i.d. (inner diameter) by Merck[®] (Merck KGaA, Darmstadt, Germany) operated at 25 °C.

The materials and methods for the mAb study can be found in detail in the work published by Eggersgluess et al. [7]. Polyethylene glycol with an average molecular weight of 400 Da (PEG 400) and NaH₂PO₄ were obtained from Merck (Darmstadt, Germany). K₂HPO₄ and Tween-20 were from Sigma Aldrich (St. Louis, MO, USA). A cell culture harvest from a Chinese hamster ovary (CHO) cell culture (harvest/cell culture harvest) was provided by Boehringer Ingelheim Pharma (Biberach, Germany). The cell culture harvest contained an IgG mAb. Size exclusion chromatography (SEC; TSKgel G3000 SWXL column; Tosoh Biosciences, Stuttgart, Germany) was performed to obtain the purity profile.

The purity P is defined in all experiments as the area of the target component peak in the ELSD chromatogram (for artemisinin) or in the size exclusion chromatogram (for the monoclonal antibody) divided by the total area of the target component and respective side components:

$$P = \frac{A_{Target\ Component}}{A_{total}} \quad (8)$$

The solvent ratio in all column experiments is defined as follows:

$$Solvent\ ratio = \frac{m_{org.}}{m_{aq.}} \quad (9)$$

The column experiments are carried out in two mini-plant columns; a stirred Kühni column (Artemisinin study) and a pulsed, packed column (mAb study). Both columns have a total volume of approximately 5 L with an effective separation height of 3.5 m. The diameter of the separating area is 26 mm. This results in an effective separation volume of about 2 L, slightly reduced by 8 vol% by the installations.

6. Conclusions

The presented work adopts the model validation workflow presented by Sixt et al. [15] and applies it to liquid-liquid extraction column modeling and simulation. Single- and multi-parameter-at-a-time studies reveal the significance of model parameters and enables the identification of combined parameter effects with support from statistical evaluation (Pareto chart and partial-least-squares loading plot). Two case studies for products from complex feed mixtures, Artemisinin and a monoclonal antibody, are presented and the comparison between simulation and experiment suggest sufficient precision and accuracy for the applied model approach to be applicable in a process development scenario. For the Artemisinin process, it is shown in the Pareto-analysis that significant parameters in regards to the concentration of the target component are the mass flow of the dispersed and continuous phase as well as the distribution coefficient of acetone. Interactions of these parameters are made visible in the partial-least-squares loading plot. It is shown that the highest concentration of Artemisinin is negatively correlated to the mass flow of the dispersed phase. Applying the validated model to the monoclonal antibody (mAb) process resulted again in model accuracy and precision comparable to the experiment. The results and procedure presented support the implementation of liquid-liquid extraction in upcoming processes, especially when feed material in the early product development is limited and traditional experiment- and pilot-testing based development strategies are not applicable.

Future research could be directed towards higher modeling depth, if experimental results suggest, that certain effects are not sufficiently described by the axial dispersion model. However, the findings shown here suggest that probably better prediction is possible by more precise model parameter determination than by an increase in model depth, which would result in more model parameters to be additionally determined.

Author Contributions: A.S. conceived, designed and performed the experiments as well as wrote the paper. All authors interpreted the data. J.S. substantively revised the work and contributed the materials and model tools. J.S. is responsible for conception and supervision.

Funding: The authors want to thank the Bundesministerium für Wirtschaft und Energie (BMWi), especially M. Gahr (Projekträger FZ Jülich), for funding this scientific work.

Acknowledgments: The authors would like to thank Reinhard Ditz/formerly Merck KGaA, Darmstadt for paper revision and discussions as well as the ITVP lab team, especially Frank Steinhäuser, Volker Strohmeyer, Thomas Knebel and Martin Kornecki for their efforts and support. Special thanks are also addressed to André Moser and Daniel Niehaus for excellent laboratory work and discussions.

Conflicts of Interest: The authors declare no conflict of interest.

Abbreviations

ADM	Axial dispersion model
CFD	Computational Fluid Dynamics
CQA	Critical quality attribute
CPP	Critical process parameter
EMA	European Medicines Agency
FDA	U.S. Food and Drug Administration
FMEA	failure-mode-effect-analysis
ICH	International Council for Harmonization of Technical Requirements for Pharmaceuticals for Human Use
LLE	Liquid-Liquid Extraction
QbD	Quality-by-Design
QTPP	Quality target product profile
PAT	Process-Analytical-Technology
PBM	Population balance model
PDA	Parenteral Drug Association
PLS	Partial-least-squares

List of Symbols

A_C	Column cross-sectional area, m^2
Bo	Bodenstein number, -
c_i^c	Concentration in the continuous phase, kg/m^3
c_i^d	Concentration in the dispersed phase, kg/m^3
$c_{i,Eq}^d$	Equilibrium concentration in the dispersed phase, kg/m^3
C_1	Constants in the axial dispersion coefficient correlation
C_2	Constants in the axial dispersion coefficient correlation
C_3	Constants in the axial dispersion coefficient correlation
d	Sauter diameter of droplets, m
D_R	Stirrer diameter, m
D_{ax}^c	Axial dispersion coefficient of the continuous phase, m^2/s
D_{ax}^d	Axial dispersion coefficient of the dispersed phase, m^2/s
H_c	Height of a mixing compartment, m
k_{eff}	Effective mass transfer coefficient, m/s
L	Column loading, $m^3/m^2/s$
N	Stirring speed, 1/s
t	Time, s

u_c	Velocity of the continuous phase, m/s
u_d	Velocity of the dispersed phase, m/s
V_c	Volume flow of the continuous phase, m ³ /s
V_d	Velocity of the dispersed phase, m ³ /s
z	Coordinate in axial direction, m
Φ	Hold-up

References

- Koch, J.; Shivelor, G. Design Principles for liquid-liquid extraction. *Chem. Eng. Prog.* **2015**, *111*, 22–30.
- Cusack, R.; Karr, A. A fresh look at liquid-liquid extraction. *Chem. Eng.* **1991**, *98*, 112.
- Kula, M.-R. Extraction and Purification of Enzymes Using Aqueous Two-Phase Systems. In *Applied Biochemistry and Bioengineering Enzyme Technology*; Academic Press: Cambridge, MA, USA, 1979; pp. 71–95, ISBN 9780120411023.
- Rosa, P.A.J.; Azevedo, A.M.; Sommerfeld, S.; Mutter, M.; Backer, W.; Aires-Barros, M.R. Continuous purification of antibodies from cell culture supernatant with aqueous two-phase systems: From concept to process. *Biotechnol. J.* **2013**, *8*, 352–362. [[CrossRef](#)] [[PubMed](#)]
- Eggersgluess, J.K.; Both, S.; Strube, J. Process development for the extraction of biomolecules application for downstream processing of proteins in aqueous two-phase systems. *Chim. Oggi/Chem. Today* **2012**, *30*, 32–36.
- Eggersgluess, J.; Wellsandt, T.; Strube, J. Integration of aqueous two-phase extraction into downstream processing. *Chem. Eng. Technol.* **2014**, *37*, 1686–1696. [[CrossRef](#)]
- Eggersgluess, J.K.; Richter, M.; Dieterle, M.; Strube, J. Multi-stage aqueous two-phase extraction for the purification of monoclonal antibodies. *Chem. Eng. Technol.* **2014**, *37*, 675–682. [[CrossRef](#)]
- Muendges, J.; Zalesko, A.; Gorak, A.; Zeiner, T. Multistage aqueous two-phase extraction of a monoclonal antibody from cell supernatant. *Biotechnol. Prog.* **2015**, *31*, 925–936. [[CrossRef](#)]
- Glatz, D.; Parker, W. Enriching liquid-liquid extraction: A step-by-step guide to evaluating and improving column efficiency. *Chem. Eng.* **2004**, *111*, 44–49.
- Buchbender, F.; Schmidt, M.; Steinmetz, T.; Pfennig, A. Simulation von Extraktionskolonnen in der industriellen Praxis. *Chem. Ing. Tech.* **2012**, *84*, 540–546. [[CrossRef](#)]
- Helling, C.; Strube, J. Quality-by-Design with Rigorous Process Modeling as Platform Technology of the Future. *Chem. Ing. Tech.* **2012**, *84*, 1334. [[CrossRef](#)]
- Yu, L.X.; Amidon, G.; Khan, M.A.; Hoag, S.W.; Polli, J.; Raju, G.K.; Woodcock, J. Understanding pharmaceutical quality by design. *AAPS J.* **2014**, *16*, 771–783. [[CrossRef](#)] [[PubMed](#)]
- Uhlenbrock, L.; Sixt, M.; Strube, J. Quality-by-Design (QbD) process evaluation for phytopharmaceuticals on the example of 10-deacetylbaccatin III from yew. *Resour. Effic. Technol.* **2017**, *3*, 137–143. [[CrossRef](#)]
- Zobel-Roos, S.; Schmidt, A.; Mestmäcker, F.; Mouellef, M.; Huter, M.; Uhlenbrock, L.; Kornecki, M.; Lohmann, L.; Ditz, R.; Strube, J. Accelerating Biologics Manufacturing by Modeling or: Is Approval under the QbD and PAT Approaches Demanded by Authorities Acceptable Without a Digital-Twin? *Processes* **2019**, *7*, 94. [[CrossRef](#)]
- Sixt, M.; Uhlenbrock, L.; Strube, J. Toward a Distinct and Quantitative Validation Method for Predictive Process Modelling—On the Example of Solid-Liquid Extraction Processes of Complex Plant Extracts. *Processes* **2018**, *6*, 66. [[CrossRef](#)]
- Alt, N.; Zhang, T.Y.; Motchnik, P.; Taticek, R.; Quarmby, V.; Schlothauer, T.; Beck, H.; Emrich, T.; Harris, R.J. Determination of critical quality attributes for monoclonal antibodies using quality by design principles. *Biologicals* **2016**, *44*, 1–15. [[CrossRef](#)] [[PubMed](#)]
- International Council for Harmonization of Technical Requirements for Pharmaceuticals for Human Use. *Quality Risk Management Q9*; ICH Harmonised Tripartite Guideline; ICH: Geneva, Switzerland, 2005.
- Treybal, R.E. Liquid extraction. *AIChE J.* **1963**, *9*, 863. [[CrossRef](#)]
- Kornecki, M.; Schmidt, A.; Strube, J. Pat as Key-Enabling Technology for QbD in Pharmaceutical Manufacturing—A Conceptual Review on Upstream and Downstream Processing. *Chem. Today* **2018**, *36*, 44–48.
- Berthelot, M.; Jungfleisch, E. On the laws that operate for the partition of a substance between two solvents. *Annales de Chimie et de Physique* **1872**, *26*, 396–407.

21. Nernst, W. Verteilung eines Stoffes zwischen zwei Lösungsmitteln und zwischen Lösungsmittel und Dampfraum. *Zeitschrift für Physikalische Chemie* **1891**, *8*, 110–139. [[CrossRef](#)]
22. Perry, R.H.; Green, D.W. *Perry's Chemical Engineers' Handbook*, 8th ed.; McGraw-Hill: New York, NY, USA, 2008; ISBN 0071422943.
23. Lewis, W.K. Laboratory and plant: The Principles of Counter-Current Extraction. *J. Ind. Eng. Chem.* **1916**, *8*, 825–833. [[CrossRef](#)]
24. McCabe, W.L.; Thiele, E.W. Graphical Design of Fractionating Columns. *Ind. Eng. Chem.* **1925**, *17*, 605–611. [[CrossRef](#)]
25. Kremser, A. Theoretical analysis of absorption process. *Natl. Pet. News* **1930**, *22*, 42.
26. Hunter, T.G.; Nash, A.W. Liquid-Liquid Extraction Systems. *Ind. Eng. Chem.* **1935**, *27*, 836–845. [[CrossRef](#)]
27. Colburn, A.P. Simplified Calculation of Diffusional Processes. *Ind. Eng. Chem.* **1941**, *33*, 459–467. [[CrossRef](#)]
28. Geankoplis, C.J.; Hixson, A.N. Mass Transfer Coefficients in an Extraction Spray Tower. *Ind. Eng. Chem.* **1950**, *42*, 1141–1151. [[CrossRef](#)]
29. Sege, G.; Woodfield, F.W. Pulse column variables. Solvent extraction of uranyl nitrate with tributyl phosphate in a 3-in.-diam. pulse column. *Chem. Eng. Prog.* **1954**, *50*, 396–402.
30. Thornton, J.D.; Logsdail, D.H. Liquid-Liquid Extraction. Part XIV.: The effect of column diameter upon the performance and throughput of pulsed plate columns. *Trans. Inst. Chem. Eng.* **1957**, *35*, 331–338.
31. Danckwerts, P.V. Continuous flow systems. *Chem. Eng. Sci.* **1953**, *2*, 1–13. [[CrossRef](#)]
32. Levenspiel, O.; Smith, W.K. Notes on the diffusion-type model for the longitudinal mixing of fluids in flow. *Chem. Eng. Sci.* **1957**, *6*, 227–235. [[CrossRef](#)]
33. Sleicher, C.A., Jr. Axial mixing and extraction efficiency. *AIChE J.* **1959**, *5*, 145–149. [[CrossRef](#)]
34. Stemerding, S.; Zuiderweg, F.J. Axial mixing and its influence on extraction efficiency. *Chem. Eng.* **1963**, *168*, 156–160.
35. Miyauchi, T.; Vermeulen, T. Longitudinal Dispersion in Two-Phase Continuous-Flow Operations. *Ind. Eng. Chem. Fundam.* **1963**, *2*, 113–126. [[CrossRef](#)]
36. Rod, V. Calculating mass transfer with longitudinal mixing. *Br. Chem. Eng.* **1966**, *11*, 483–487.
37. Steiner, L.; Hartland, S. Modellierung von Extraktionskolonnen unter Anwendung der Ruckvermischungstheorie. *Chem. Ing. Tech.* **1980**, *52*, 602–603. [[CrossRef](#)]
38. Reissinger, K.-H. Vermischung und Konzentrationsprofile in pulsierten Siebboden-Extraktoren. *Chem. Ing. Tech.* **1982**, *54*, 1070–1071. [[CrossRef](#)]
39. Jiříčný, V.; Krátký, M.; Procházka, J. Counter-current flow of dispersed and continuous phase—I. *Chem. Eng. Sci.* **1979**, *34*, 1141–1149. [[CrossRef](#)]
40. Jiříčný, V.; Krátký, M.; Procházka, J. Counter-current flow of dispersed and continuous phase—II. *Chem. Eng. Sci.* **1979**, *34*, 1151–1158. [[CrossRef](#)]
41. Casamatta, G.; Vogelpohl, A. Modellierung der Fluidodynamik und des Stoffübergangs in Extraktionskolonnen. *Chem. Ing. Tech.* **1984**, *56*, 230–231. [[CrossRef](#)]
42. Haverland, H.; Vogelpohl, A.; Gourdon, C.; Casamatta, G. Simulation of fluid dynamics in a pulsed sieve plate column. *Chem. Eng. Technol.* **1987**, *10*, 151–157. [[CrossRef](#)]
43. Al Khani, S.D.; Gourdon, C.; Casamatta, G. Simulation of hydrodynamics and mass transfer of disks and rings pulsed column. *Ind. Eng. Chem. Res.* **1988**, *27*, 329–333. [[CrossRef](#)]
44. Cruz-Pinto, J.J.C.; Korchinsky, W.J. Drop breakage in counter current flow liquid-liquid extraction columns. *Chem. Eng. Sci.* **1981**, *36*, 695–703. [[CrossRef](#)]
45. Coulaloglou, C.A.; Tavlarides, L.L. Description of interaction processes in agitated liquid-liquid dispersions. *Chem. Eng. Sci.* **1977**, *32*, 1289–1297. [[CrossRef](#)]
46. Tavlarides, L.L.; Bapat, P.M. *Models for Scale-Up of Dispersed Phase Liquid-Liquid Reactors*; AIChE Symposium Series; American Institute of Chemical Engineers: New York, NY, USA, 1984; p. 238.
47. Hamilton, J.A.; Pratt, H.R.C. Droplet coalescence and breakage rates in a packed liquid extraction column. *Am. Inst. Chem. Eng. J.* **1984**, *30*, 442–450. [[CrossRef](#)]
48. Kronberger, T.; Ortner, A.; Zulehner, W.; Bart, H.J. Numerical simulation of extraction columns using a drop population model. *Comput. Chem. Eng.* **1995**, *19*, 639–644. [[CrossRef](#)]
49. Henschke, M.; Pfennig, A. Simulation of packed extraction columns with the REDROP model. In Proceedings of the 12th International Congress of Chemical and Process Engineering, CHISA '96, Praha, Czech Republic, 25–30 August 1996.

50. Hoting, B. Untersuchungen zur Fluidodynamik und Stoffübertragung in Extraktionskolonnen mit Strukturierten Packungen. Ph.D. Thesis, Clausthal-Zellerfeld, Technology University, Clausthal-Zellerfeld, Germany, 1995.
51. Bart, H.-J.; Garthe, D.; Grömping, T.; Pfennig, A.; Schmidt, S.; Stichlmair, J. Vom Einzeltropfen zur Extraktionskolonne. *Chem. Ing. Tech.* **2006**, *78*, 543–547. [[CrossRef](#)]
52. Jildeh, H.; Attarakih, M.; Bart, H.-J. Simulation von Extraktionskolonnen mit LLECMOD. *Chem. Ing. Tech.* **2012**, *84*, 1282. [[CrossRef](#)]
53. Ayesterán, J.; Kopriwa, N.; Buchbender, F.; Kalem, M.; Pfennig, A. ReDrop—A Simulation Tool for the Design of Extraction Columns Based on Single-Drop Experiments. *Chem. Eng. Technol.* **2015**, *38*, 1894–1900. [[CrossRef](#)]
54. Franke, M.; Górak, A.; Strube, J. Auslegung und Optimierung von hybriden Trennverfahren. *Chem. Ing. Tech.* **2004**, *76*, 199–210. [[CrossRef](#)]
55. Leistner, J. Modellierung und Simulation Physikalischer, Dissoziativer und Reaktiver Extraktionsprozesse. Ph.D. Thesis, Dortmund University, Dortmund, Germany, 2004.
56. Wellsandt, T.; Stanisch, B.; Strube, J. Development of Micro Separation Technology Modules. Part 1: Liquid-Liquid Extraction. *Chem. Ing. Tech.* **2015**, *87*, 1198–1206. [[CrossRef](#)]
57. Hlawitschka, M.W. Computational Fluid Dynamics Aided Design of Stirred Liquid-Liquid Extraction Columns. Ph.D. Thesis, TU. Kaiserslautern, Kaiserslautern, Germany, 2013.
58. Steinmetz, T. Tropfenpopulationsbilanzgestütztes Auslegungsverfahren zur Skalierung einer Gerührten Miniplant-Extraktionskolonne. Ph.D. Thesis, Kaiserslautern Technology University, Kaiserslautern, Germany, 2007.
59. Kolb, P. Hydrodynamik und Stoffaustausch in einem gerührten Miniplantextraktor der Bauart Kühni. Ph.D. Thesis, Kaiserslautern Technology University, Kaiserslautern, Germany, 2004.
60. Breysee, J.; Bühlmann, U.; Godfrey, J.C. Axial Mixing Characteristics of Industrial and Pilot Scale Kühni Columns. *AIChE Symp. Ser.* **1983**, *8*, 94–101.
61. Steiner, L.; Kumar, A.; Hartland, S. Determination and correlation of axial-mixing parameters in an agitated liquid-liquid extraction column. *Can. J. Chem. Eng.* **1988**, *66*, 241–247. [[CrossRef](#)]
62. Rod, V.; Misek, T. Stochastic modelling of dispersion formation in agitated liquid-liquid systems. *Trans. Inst. Chem. Eng.* **1982**, *60*, 48–57.
63. Bauer, R. Die Längsvermischung beider Phasen in einer gerührten Fest-Flüssig Extraktionskolonne. Ph.D. Thesis, RTH, Zürich, Switzerland, 1976.
64. Rod, V. Calculation of Extraction Columns with Longitudinal Mixing. *Briti. Chem. Eng.* **1964**, *9*, 300–304.
65. Wolschner, B.; Sommeregger, E.; Marr, R. Die Berechnung des Konzentrationsprofils in einem Drehscheibenextraktor - Bauart RDC. *Chem. Ing. Tech.* **1980**, *52*, 277. [[CrossRef](#)]
66. Schmidt, A.; Strube, J. Application and Fundamentals of Liquid-Liquid Extraction Processes: Purification of Biologicals, Botanicals, and Strategic Metals. In *Kirk-Othmer Encyclopedia of Chemical Technology*; John Wiley & Sons, Inc.: Hoboken, NJ, USA, 2018. [[CrossRef](#)]
67. Hoting, B.; Vogelpohl, A. Untersuchungen zur Fluidodynamik und Stoffübertragung in Extraktionskolonnen mit strukturierten Packungen Teil I: Fluidodynamisches Verhalten in Abhängigkeit von Energieeintrag und Phasenverhältnis. *Chem. Ing. Tech.* **1996**, *68*, 105–109. [[CrossRef](#)]
68. Gronemeyer, P.; Ditz, R.; Strube, J. DoE based integration approach of upstream and downstream processing regarding HCP and ATPE as harvest operation. *Biochem. Eng. J.* **2016**, *113*, 158–166. [[CrossRef](#)]
69. Schmidt, A.; Sixt, M.; Huter, M.; Mestmäcker, F.; Strube, J. Systematic and Model-Assisted Process Design for the Extraction and Purification of Artemisinin from *Artemisia annua* L.—Part II: Model-Based Design of Agitated and Packed Columns for Multistage Extraction and Scrubbing. *Processes* **2018**, *6*, 179. [[CrossRef](#)]

